Green Chemistry

PAPER

Cite this: *Green Chem.*, 2020, **22**, 2036

Producing high yield of levoglucosan by pyrolyzing nonthermal plasma-pretreated cellulose†

Lusi A,[a] Haiyang Hu[b] and Xianglan Bai*[a]

Atmospheric pressure nonthermal plasma treatment can be a novel, green and low energy method to convert biomass to biobased chemicals. The unique physiochemistry of plasma discharge enables reactions within biomass that otherwise could not possibly occur under traditional conditions. In this study, we present a simple method of producing a high yield of levoglucosan from cellulose without using any catalysts, chemicals, solvents or vacuum, but by using plasma treatment to control the depolymerization mechanism of cellulose. Cellulose was first pretreated in a dielectric barrier discharge reactor operating in ambient air or argon for 10–60 s, followed by pyrolysis at 350–450 °C to produce up to 78.6% of levoglucosan. Without the plasma pretreatment, the maximum yield of levoglucosan from cellulose pyrolysis was 58.2%. The results of this study showed that the plasma pretreatment led to homolytic cleavage of glycosidic bonds. The resulting free radicals were then trapped within the cellulose structure when the plasma discharge stopped, allowing subsequent pyrolysis of the plasma-pretreated cellulose to proceed through a radical-based mechanism. The present results also revealed that although the radical-based mechanism is highly selective to levoglucosan formation, this pathway is usually discouraged when the untreated cellulose is pyrolyzed due to the high energy barrier for homolytic cleavage. Initiating homolytic cleavage during the plasma pretreatment also helped the pretreated cellulose to produce higher yields of levoglucosan using lower pyrolysis temperatures. At 375 °C, the levoglucosan yield was only 53.2% for the untreated cellulose, whereas the yield reached 77.6% for the argon-plasma pretreated cellulose.

Received 20th January 2020,
Accepted 28th February 2020

DOI: 10.1039/d0gc00255k

rsc.li/greenchem

Introduction

Cellulose is the most abundant biopolymer on Earth, accounting for 40–50% of lignocellulosic biomass. Cellulose is also an important feedstock in biorefineries for biofuels and chemicals.[1,2] Producing biochemicals from cellulose and cellulosic biomass is particularly attractive. By this method, not only petroleum-derived chemicals, but also chemicals with unique properties that are difficult to produce from typical petroleum feedstocks can be produced.[3] Although promising, producing bio-based chemicals in a cost-competitive way remains a significant challenge. Among the approaches to improve the competitiveness of biobased chemicals are increasing the product yields and reducing production costs. Ideally, a high yield of the targeted molecule is obtained using a simple process and mild conditions with the reduced use of costly catalysts, solvents or enzymes. This goal is often difficult to achieve based on traditional methods. However, the application of nonthermal plasma technology on biomass could provide an opportunity to achieve this goal.

Nonthermal plasma-based conversion is unique as it uses an unconventional approach for more efficient and potentially low-cost processing.[4,5] Plasma is ionized gas containing electrons, radicals, ions, atoms and molecules, usually produced when a high electric field is applied to a neutral gas.[6] Plasma is classified as either equilibrium plasma or non-equilibrium plasma. In equilibrium plasma, also called thermal plasma, the electrons and other heavier species reach thermal equilibrium. The gas temperature can reach several thousands of degrees in thermal plasma, reflecting high energy consumption. On the other hand, non-equilibrium plasma can be produced using lower amounts of energy since the temperature of electrons alone is much higher than the temperatures of other heavier species. Non-equilibrium plasma is also called nonthermal plasma as the macroscopic temperature of the plasma discharge system can be at or near room temperature. Since nonthermal plasma creates a chemically rich environment at low temperatures, it was previously employed in surface treat-

[a]*Department of Mechanical Engineering, Iowa State University, Ames, IA 50011, USA. E-mail: bxl9801@iastate.edu*

[b]*Department of Aerospace Engineering, Iowa State University, Ames, IA 50011, USA*

†Electronic supplementary information (ESI) available. See DOI: 10.1039/d0gc00255k

ment, wastewater treatment and sterilization, used as a green and low-energy technology.[7,8] When the nonthermal plasma is applied to biomass, high-energy electrons accelerated by a strong electric field collide with the feed gas and biomass molecules, causing ionizations and homolytic bond dissociations independent of the temperature of the system. Furthermore, the active species in the plasma discharge could also interact with biomass molecules for additional reactions. As a result, various reactions that otherwise could not occur at low temperatures or without the use of a catalyst become possible. For example, nonthermal plasma treatment is able to delignify biomass at room temperature in the absence of acid or solvent.[5] Since inhibitory compounds were suppressed in the absence of acid, the enzymatic digestibility was also improved for the plasma-pretreated biomass.[9,10] Nonthermal plasma was also used to improve the hydrolyzability of cellulose or applied to catalytic pyrolysis of biomass or catalytic upgrading of bio-oil to promote hydrodeoxygenation and reduce catalytic coke.[11–14] Nonthermal plasma is highly versatile, as the chemical composition of plasma discharge and its density are influenced by the power supply, plasma actuator configuration, the feed gas type, and the feedstock materials. Moreover, using nonthermal plasma can be an attractive option for promoting greener production of bioenergy. While only electricity is required to generate plasma, abundant renewable electricity can also be used.

In the present study, we report a nonthermal plasma-assisted method that is able to produce high yields of levoglucosan (LG) from cellulose in the absence of catalysts, chemicals, solvents or vacuum. LG is known as a high-value, biomass-derived chemical.[15] It is an anhydroglucose monomer, which can be hydrolyzed to glucose or directly fermented to alcohol and lipids.[16,17] LG also has applications in the syntheses of pharmaceutical chemicals, biodegradable plastics, and surfactants.[18] LG is usually produced from cellulose or cellulosic biomass by pyrolysis, but it can also be produced by converting cellulose in hot and compressed aprotic solvents.[18–21] Although it is the primary product of cellulose depolymerization, improving LG yield has been a bottleneck for decades.[18,22,23] In this study, we discovered that the combination of nonthermal plasma pretreatment and subsequent pyrolysis is a simple and effective method to increase LG yield.

Materials and methods

Materials

Avicel microcrystalline cellulose was purchased from Sigma-Aldrich. LG was purchased from Carbon-synth, cellobiose was from Fluka Analytical, and cellobiosan was from Alfa Aesar. Glucose and dimethyl sulfoxide (DMSO) were purchased from Fisher Scientific, and hydroquinone was from Acros Organics.

Plasma pretreatments

Nonthermal plasma treatments were carried out using a dielectric barrier discharge (DBD) reactor consisting of two parallel copper plate-electrodes separated by a polycarbonate block as a dielectric material. For the power supply, a high-voltage AC power amplifier (Trek Model 20/20C) and a sweep function generator (B&K PRECISION 4017A) were used. The voltage and current signals were monitored using an oscilloscope (Tektronix MDO3102 mixed domain). Each time, about 20 mg of the sample was treated in ambient air or using room temperature argon (Ar). During the pretreatments, the AC power voltage, frequency and treatment time were parameters. The temperature distribution of cellulose inside the DBD reactor was analyzed using a high-speed infrared (IR) thermal imaging system (FLIR A615) through an IR window (FLIR IR Window-IRW).

Pyrolysis tests

Fast pyrolysis was carried out using a Frontier micro-pyrolyzer system with an auto-shot sampler (Rx-3050 TR, Frontier Laboratories, Japan) and a single-stage furnace oven. During pyrolysis, a deactivated stainless-steel cup containing approximately 0.25 mg of the sample was dropped into a preheated furnace. Helium gas was used as both the sweep gas and carrier gas. The vapors exiting the pyrolyzer were directly carried into a gas chromatogram (GC, Agilent 7890A) for online characterization of the products. The front inlet temperature at the GC was kept at 250 °C to prevent condensation of the vapor products. The GC oven was initially kept at 40 °C and then ramped up to 280 °C at a heating rate of 6 °C min^{-1}. Two identical capillary columns (ZB-1701, 60 m × 250 μm × 0.25 μm) were separately connected to a mass spectrometer (MS, Agilent 5975C) and flame ionization detector (FID). A Porous Layer Open Tubular (PLOT) column (60 m × 0.320 mm) (GS-GasPro, Agilent, USA) was connected to a thermal conductivity detector (TCD). The compounds identified from the MS were quantified in the FID. The calibration curve was created by injecting different concentrations of LG into the GC. Non-condensable gases, were analyzed with the TCD using the standard gas mixture. The pyrolysis temperature was 450 °C for most cases unless specified. Each pyrolysis case was triplicated for reproducibility. In the case of co-pyrolysis with hydroquinone, 0.25 mg of a saccharide sample was mixed with 0.1 mg of hydroquinone. The plasma pretreated samples were pyrolyzed within 15 minutes after the plasma pretreatment unless indicated.

SEM analysis

The microstructures of the samples were examined using a scanning electron microscope (SEM, Quanta-FEG 250, FEI) at a 10 kV accelerating voltage. Segments of the samples were mounted onto double-stick carbon tape on a 45° incline. The samples were coated with 5 nm of iridium for conductivity.

XRD measurements

X-ray powder diffraction (XRD) analysis was performed on a Siemens D500 X-ray diffractometer using a Cu X-ray tube (λ = 0.154 nm), operating at 45 kV and 30 mA. The 2θ was measured from 5° to 40°, with a scanning speed of 1° min^{-1}.

The crystallinity of cellulose was defined as the ratio of the peak areas assigned to crystalline cellulose to the total peak area.

Solubility tests

The solubility of samples in the DMSO solution was determined by dissolving 100 mg of cellulose samples in 10 mL of DMSO at room temperature overnight. The insoluble solvent fraction was centrifuged and vacuum-dried before its weight was measured.

LC-MS analysis

The plasma-treated cellulose was dispersed in deionized water and centrifuged to extract the water-soluble fraction. Negative ion mode electrospray mass spectra were obtained using an Agilent QTOF 6540 MS. An Agilent LC 1200 series system equipped with an autosampler was used. One microliter of the sample (concentration of approximately 10 ppm) was injected into a JetStream ESI ion source. The mass range was kept constant from 100 to 1000 amu. The instrument was operated in the 4 GHz HiRes mode. Accurate mass measurement was achieved by constantly infusing a calibrant (masses: 112.9855 and 966.0007). The samples were separated using a Thermo ACCLAIM HILIC-10 (3 μm, 120 A, 4.6 × 150 mm) column. Water (0.1% formic acid) and acetonitrile were used as effluents for LC separation. Acetonitrile was maintained at 90% for 4 min, then ramped to 93% and maintained for 10 min. The flow rate was constant at 1 mL min^{-1}.

TGA

Thermogravimetric analysis (TGA) was conducted using a Mettler Toledo TGA/DSC 1 instrument. About 10 mg of the sample was heated from room temperature to 600 °C at a heating rate of 10 °C min^{-1} using nitrogen gas with a flow rate of 100 mL min^{-1}.

FTIR analysis

Fourier Transform Infrared (FTIR) analysis was conducted using a Thermo Scientific Nicolet iS10 equipped with a Smart iTR accessory. The wavenumbers ranged from 750 cm^{-1} to 4000 cm^{-1} and each sample was scanned 32 times at a resolution of 4 cm^{-1} and an interval of 1 cm^{-1}.

Electrostatic elimination

A Mettler Toledo 63052302 Haug deionizer was used to remove static electricity from the samples.

EPR analysis

Electron paramagnetic resonance (EPR) spectra were recorded on a Bruker ELEXYS E580 FT-EPR spectrometer at the X-band microwave frequency (9.5 GHz) with a magnetic field modulation of 100 kHz at room temperature. EPR parameters were as follows: center field of 3355 G, sweep width of 200 G, power of 1.982 mW, sweep time of 20.97 s, receiver gain of 50 dB, modulation amplitude of 5 G, and modulation frequency of 100 kHz. The plasma-pretreated samples were analyzed within 30 minutes after the pretreatments unless otherwise indicated.

Results and discussion

Plasma pretreatment of cellulose

The typical electric voltage–current graph during the plasma treatment is given in Fig. S1.† The spiked form of the current indicates plasma formation. The power input during the plasma treatment was 2.1–2.3 W. According to the IR thermographic image shown in Fig. S2,† the temperatures of cellulose and the plasma discharge remain near room temperature. After the plasma treatments, the pretreated cellulose was nearly entirely recovered in its original solid form (*i.e.*, the mass recovery >99.9%).

Pyrolysis of the plasma-pretreated cellulose

The pretreated cellulose was then immediately pyrolyzed at 450 °C to produce LG. In this study, the LG yield from the untreated cellulose pyrolyzed at the same temperature was 57.2%, which is in accordance with a previously reported study.[24] LG yields obtained from the Ar plasma-pretreated cellulose are shown in Fig. 1(a) and (b) as a function of plasma treatment time. For the tests shown in Fig. 1(a), the pretreatments were carried out by fixing the AC frequency at 2 kHz and changing the voltages. With different voltages, the LG

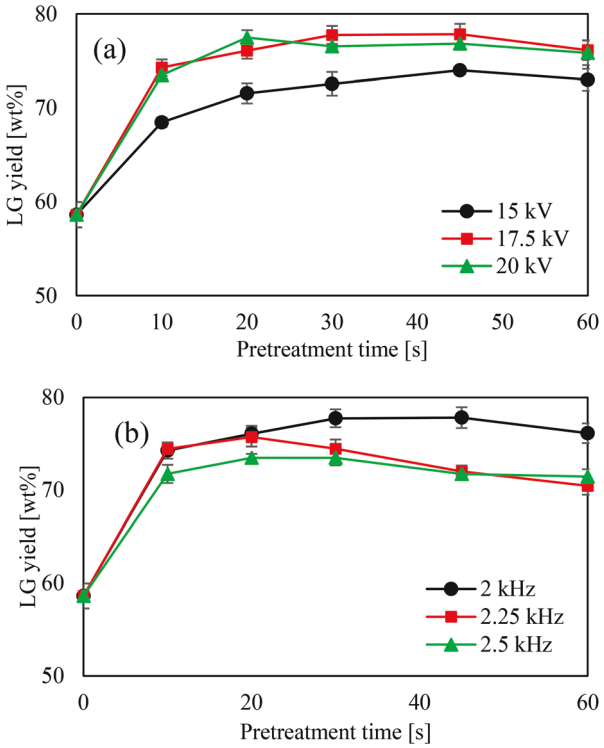

Fig. 1 LG yield obtained from pyrolysis of the Ar plasma-pretreated cellulose as a function of the pretreatment time. The AC power conditions during the pretreatments are: (a) f = 2 kHz and (b) V = 17.5 kV.

yield first increased with increasing pretreatment time and then either plateaued or started to decrease from the corresponding maximum values with prolonged pretreatment times. The optimum LG yield was 74% when the voltage was 15 kV, obtained with a pretreatment time of 45 s. When the voltage increased to 17.5 kV, the optimum LG yield and pretreatment time were 77.9% and 30 s, respectively. Further increasing the voltage had no effect on the optimum LG yield, but the corresponding pretreatment time reduced to 20 s. For the pretreatment conditions in Fig. 1(b), the AC voltage remained at 17.5 kV and the frequency varied between 2 kHz and 2.5 kHz. AC frequencies lower than 2 kHz were not studied because it was difficult to obtain plasma discharge at the lower frequencies in this study. The optimum LG yields, obtained with a treatment time of 20 s, were 75.8% and 73.5% for the pretreatment frequencies of 2.25 kHz and 2.5 kHz, respectively.

The LG yields obtained from pyrolysis of the air plasma-pretreated cellulose are given in Fig. 2(a) and (b). In Fig. 2(a), the AC frequency was kept at 2 kV during the plasma pretreatment. When the voltage was 15 kV, the optimum LG yield and pretreatment time were 73.8% and 45 s, respectively. Similar to that which was observed with the Ar plasma pretreatment, increasing the voltage to 17.5 kV also increased the optimum LG yield (to 75.5%) and shortened the corresponding pretreatment time (to 30 s). However, the optimum LG yield was only 66.6% when the voltage further increased to 20 kV. In Fig. 2(b), the AC voltage was fixed at 15 kV during the plasma pretreatment. The corresponding optimum LG yields were 75% and 73% for the frequencies of 2.25 kV and 2.5 kV, respectively, and the pretreatment times were both 20 s. Overall, the plasma pretreatment of cellulose was highly effective at increasing the LG yield during pyrolysis. The Ar plasma-pretreatment was slightly more effective than the air plasma-pretreatment, delivering higher and more stable LG yields. In either type of the pretreatments, moderate voltage and frequency were favored for producing higher LG yields. A higher AC voltage or frequency corresponds to increased plasma discharge power.

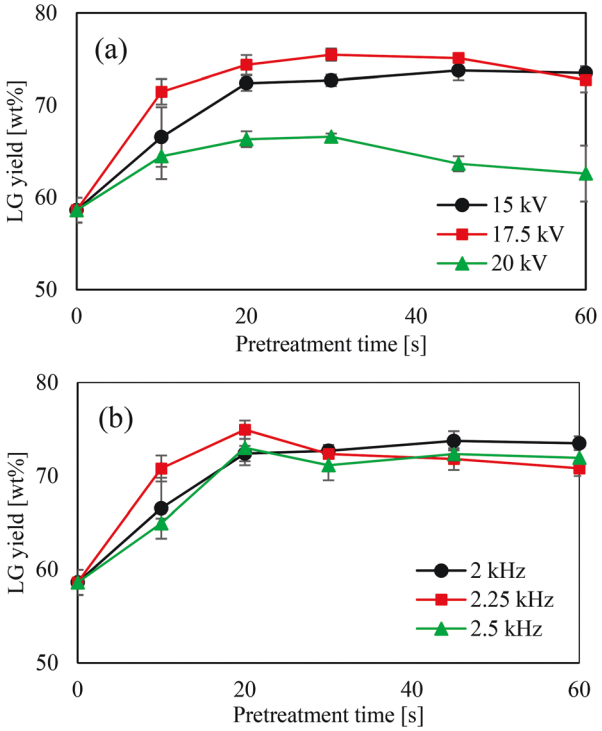

Fig. 2 LG yield obtained from pyrolysis of the air plasma-pretreated cellulose as a function of the pretreatment time. The AC power conditions during the pretreatments are: (a) f = 2 kHz and (b) V = 15 kV.

During the cellulose pyrolysis tests, other condensable vapor products (such as furans, furfurals, acetol, and anhydrosugars), char and gases (mainly CO and CO_2) were also produced. While char and non-volatile condensable products could not be collected for analysis, the GC/MS-TCD analysis of the pyrolysis vapors showed that the increase of LG yield with the plasma-pretreated cellulose compared to the untreated cellulose was always accompanied by the decrease in the yields of furans, furfurals, acetol, CO and CO_2. Since these oxygenated products are derived from the glycosidic-ring opening reactions, the increased LG yield inhibited their formation. On the other hand, the yield of 1,6-anhydro-β-D-glucofuranose (*i.e.*, the isomer of LG) increased slightly with increasing LG yield.

Cellulose pyrolysis mechanism and the effect of plasma pretreatment

As shown above, plasma pretreatment is a simple, green and effective method to increase LG production from cellulose pyrolysis. The primary question to be investigated in this study is why such a simple pretreatment of cellulose could dramatically increase LG production, enabling an unprecedentedly high LG yield.[18,22,23]

Cellulose is a polysaccharide, in which hundreds to thousands of glucose units are linearly connected by 1,4-β-glycosidic bonds. While LG is the primary product of cellulose pyrolysis, the exact mechanisms of cellulose pyrolysis and LG formation are not well known. To date, numerous studies have investigated the topic and there are still significant controversies and uncertainties.[23–32] According to a lumped reaction kinetic model, cellulose first converts to an unknown intermediate called active cellulose, and then further converts to gases, char, and volatiles.[26,32] The liquid intermediates formed during cellulose pyrolysis were captured and found to be composed of anhydro-oligosaccharides with various degrees of polymerization (DPs).[26,27,33] Therefore, it was proposed in later studies that, initially, cellulose is randomly cleaved at the midchain to form cellulose chain fragments with lower DPs and the fragments are further decomposed to LG and other products.[28] However, these reaction models do not reveal the detailed mechanisms of glycosidic bond cleavage and LG formation from cellulose chains. Transglycosylation offers the most plausible explanation of how LG is formed from cellulose, and according to it, a 1,4-glycosidic bond cleavage and a new bridge bond between C1 and C6 lead to the formation of LG. Proposed routes for transglyco-

sylation further include homolytic, heterolytic, and concerted mechanisms.[22,29–31,34,35] In their previous study, Mayes and Broadbelt calculated activation energies and reaction rates of the three proposed mechanisms using density functional theory and reported that the energy barriers for both the homolytic and heterolytic mechanisms are much higher than that of the concerted mechanism, in which the glycosidic bond is cleaved at the same time that the C1 and C6 bridge of LG is formed.[22] According to their proposed concerted mechanism, an initial concerted glycosidic cleavage in a midchain would produce a cellulose-like polymer with a LG chain end and a shorter cellulose chain. In subsequent depropagation steps, a LG molecule is released from the LG chain end, followed by the scission of a glycosidic bond. The effect of hydrogen bonding in the cellulose network has also been investigated previously.[36,37] A recent study by Maliekkal *et al.* suggested that in a low-temperature region, vicinal hydroxyl groups between cellulose sheets can significantly lower the activation barriers of transglycosylation through a catalytic effect.[38] According to the study, the activation energy of the hydroxyl-catalyzed transglycosylation is even lower than that of the concerted mechanism.

Despite the fact that these previously proposed mechanisms suggest several plausible pathways for forming LG from cellulose, experimentally achieving high yields of LG has been the bottleneck. The reported LG yields vary significantly, depending on reactor configuration, pyrolysis parameters and feedstock conditions used in individual studies.[18] For example, inorganic impurities can suppress LG formation due to a catalytic effect.[39] In previous studies, higher LG yields were often obtained when pure crystalline cellulose was fast pyrolyzed at a temperature range of 400–500 °C. Devolatilization of cellulose usually does not start at temperatures below 350 °C. It was also important to reduce heat and mass transfer limitations in the solid and liquid phases during pyrolysis or limit secondary reactions of LG in the vapor phase.[40–42] However, even with these nearly ideal experimental conditions that supposedly promote LG formation, the LG yield could hardly exceed 60% under atmospheric pressure conditions.[24,40–43]

In the present study, both the untreated cellulose and plasma-treated cellulose were pyrolyzed using the same pyrolyzer and identical operating conditions. Thus, the increased LG yields were not related to the reactor configuration, pyrolysis parameters and secondary reactions in the vapor phase. The effect of the impurity content can also be excluded since the plasma-pretreated cellulose was directly pyrolyzed without any additional procedures. Thus, the plasma-pretreated cellulose was carefully evaluated in the following sections to determine the role of plasma pretreatment on cellulose and cellulose pyrolysis.

The microstructure of plasma-treated cellulose

Previous studies suggest that LG yield can be sensitive to the dimensions of cellulose samples due to heat and mass transfer limitations.[43,44] Accordingly, changes in the particle size or microstructure of the plasma-pretreated cellulose compared to those of untreated cellulose could affect the LG yield during subsequent pyrolysis. In this study, however, there was no apparent change in either the particle size or the appearance of cellulose after the plasma treatments. The SEM images (Fig. S3†) also confirm no change in the microstructure of cellulose after the plasma pretreatment. Therefore, the increased LG yield was not related to the physical properties of the pretreated cellulose or its heat and mass transfer conditions.

Solubility and degree of polymerization

It has previously been reported that nonthermal plasma treatment increases cellulose solubility and reduces the DP of cellulose chains.[5,13] In this study, the solubility of cellulose in a DMSO solution increased from 43% for the untreated cellulose to 55.1% for the air plasma-treated cellulose, and 58.4% for the Ar plasma-treated cellulose, which are in agreement with previous findings (pretreatment conditions are 15 kV, 2 kHz and 30 s for "the air plasma-treated cellulose", and 17.5 kV, 2 kHz and 30 s for "the Ar plasma-treated cellulose"; same conditions in the following sections unless specified). To further understand the solubility change, the water-soluble fraction of the plasma-treated cellulose was analyzed by LC-MS. While the plasma-treated cellulose was mostly insoluble in water, anhydro-oligosaccharides and oligosaccharides with DP up to 4 (*i.e.*, m/z = 342, 324, 486, 504, 648, 666) could be detected from the water solutions (Fig. S4†). This result implies that the plasma treatment caused the glycosidic bond cleavage to reduce the DP of the cellulose chain.[14] It has previously been documented that LG yield is negatively correlated with the length of a glycosidic chain because it is difficult to produce LG from the reducing end of the chain.[45,46] According to the theory, the plasma-pretreated cellulose with a reduced DP supposedly produces lower LG yields than the untreated cellulose during pyrolysis. Therefore, the changes in the cellulose DP by plasma pretreatment also cannot explain the increase of LG.

Crystallinity

Increased solubility of cellulose could also be related to a decrease of crystallinity. Crystallinities of the untreated and plasma-treated cellulose were analyzed and the XRD results are given in Fig. 3. The crystallinity index decreased after the plasma treatment from 0.621 for the untreated cellulose to 0.586 for the Ar plasma-treated cellulose and 0.601 for the air plasma-treated cellulose. The crystallinity decrease could be associated with the increase of amorphous cellulose or the glycosidic bond cleavage in the crystalline region of cellulose during the plasma treatment. It was suggested that a high crystallinity of cellulose is favorable for LG production.[36,47] However, this statement was challenged in other studies where researchers saw no effect of cellulose crystallinity on LG yield.[18,46] Regardless of which statement is accurate, neither of them can explain the increase of LG yield in this study. In Fig. 3, a small peak with a 2θ of 20.5° newly found in the Ar plasma-treated cellulose is indicative of a cellulose II structure. Transformation of cellulose I to cellulose II is usually observed

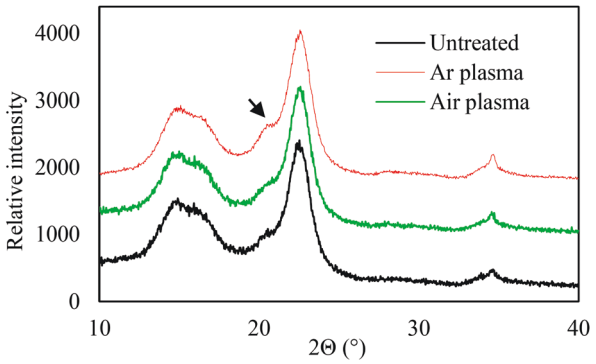

Fig. 3 XRD results of the untreated and plasma-treated cellulose. The AC power conditions and pretreatment time are f = 17.5 kV, V = 2 kHz and t = 30 s for the Ar plasma-treated cellulose, and f = 15 kV, V = 2 kHz and t = 30 s for the air plasma-treated cellulose.

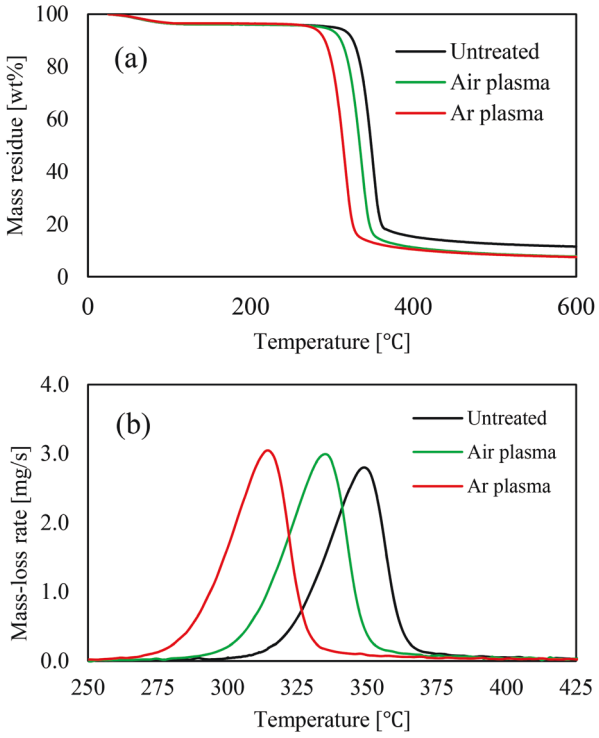

Fig. 4 TGA analysis of the untreated and pretreated cellulose. (a) TGA profile and (b) DTG curve. The AC power conditions and pretreatment time are f = 17.5 kV, V = 2 kHz and t = 30 s for the Ar plasma-treated cellulose, and f = 15 kV, V = 2 kHz and t = 30 s for the air plasma-treated cellulose.

when natural cellulose is regenerated or treated in an alkaline solution. It was suggested that the microfibrils of the swelled cellulose intermingle to transform the parallel chain packing in cellulose I to the antiparallel chain packing for the cellulose II structure.[48] According to an alternative theory, the transition from cellulose I to cellulose II is caused by changes in the chain conformation.[49] Since neither cellulose dissolution nor swelling could occur in this study during the plasma treatment, changing the chain conformation through rotating C6-OH in the cellulose provides a better explanation of how the cellulose II structure formed.

Thermal stability

Thermal stabilities of the untreated and plasma-treated cellulose are evaluated using TGA. In Fig. 4(a) and (b), both the thermal decomposition temperature and the temperature corresponding to the maximum mass loss rate were lower for the plasma-treated cellulose compared to those of the untreated cellulose. As seen in Fig. 4(b), the temperature for the maximum mass loss rate was 351 °C for the untreated cellulose, 336 °C for the air plasma-treated cellulose, and 315 °C for the Ar plasma-treated cellulose. The shifts in the temperatures were also accompanied by the increased intensities of the mass-loss rates and decreased char in the pretreated cellulose. As seen in Fig. 4(a), the yield of char at 600 °C was 11.5% for the untreated cellulose, whereas it was only 7.5% for both the air plasma-treated and Ar plasma-treated cellulose. Since the major volatile product during cellulose pyrolysis is LG and the increase of LG reduces char yield and other light oxygenates, the TGA results support the pyrolysis results described above. Moreover, the shift in the TGA temperatures also suggests that the plasma-pretreated cellulose is more readily depolymerized at lower pyrolysis temperatures using lower amounts of energy. Amorphous cellulose usually decomposes at lower temperatures than crystalline cellulose since the rigid and well-organized structure of the crystalline cellulose is harder to decompose. However, amorphous cellulose does increase LG production during pyrolysis. Also, it usually produces higher amounts of char than crystalline cellulose.[47] Therefore, the observed changes in the TGA profiles are not caused by increasing amorphous cellulose.

Functional groups

FTIR analysis was also carried out to compare the functional groups of the untreated and plasma-treated cellulose (Fig. S5†). Nonthermal plasma treatment is a popular method for surface treatments since it is capable of changing the surface functionalities of a material. For example, plasma treatments could change the hydrophobicity of cellulose fibers.[50–52] When plasma discharge occurs in air, the electron collisions with oxygen molecules can produce ozone and oxygen radicals. Hydroxy radicals could also be produced by plasma discharge if moisture is present. These species are known as strong oxidation agents. In this study, no significant changes in the IR bonds were found between the FTIR spectra of the untreated and plasma-treated cellulose, other than the peak intensity of the glycosidic bond at 1157 cm^{-1} slightly decreasing in the plasma-treated cellulose. This decrease is likely due to the cleavage of the glycosidic bond described above. The IR band of the carbonyl bond was not observed at 1750 cm^{-1}, suggesting that the oxidation reaction was insignificant, probably due to the short pretreatment times. Oxidations are non-selective and can cause ring-opening reactions. Therefore, the LG yield should have decreased in this

study if oxidations were the major reaction occurring during the plasma pretreatment.

Free electron and ion formation by plasma discharge

The plasma-pretreated cellulose samples were found to be statically charged when they were freshly treated. The static charge is caused by an imbalance between positive and negative ions within or on the surface of a material. During plasma discharge, electrons are ripped away from molecules and atoms, forming free electrons and positively charged ions. To determine the effect of free electrons or ions that remain on the pretreated cellulose, the freshly treated cellulose was first neutralized by using an electric deionizer and then pyrolyzed. If the increase of the LG yield observed in this study is associated with the electrical charge, the LG yield should decrease substantially after the neutralization. However, over 74% of LG yield was obtained from the neutralized cellulose, suggesting that free ions and electrons are not the primary reason for the increased LG yield.

Formation of long-lived free radicals

Free radical formation due to homolytic cleavage is an important feature of plasma discharge. When high-energy free electrons collide with neutral molecules, the molecules could reach an excited state due to the energy transferred from the electrons. The energy levels of the excited molecules could become high enough to overcome the barrier for homolytic cleavage. For example, the energy density of electrons is 1–10 eV in a DBD reactor with an electric field of 0.1–100 kV cm^{-1} operating at atmospheric pressure.[53] The energies at this range are higher than the dissociation energies of various organic bonds. Reactive free radicals are usually difficult to detect experimentally because of their extremely short lifetimes. However, there are also long-lived free radicals that can be captured by radical spin-trapping techniques, such as EPR. The EPR spectra of the fresh Ar plasma-treated cellulose and the fresh air plasma-treated cellulose are given in Fig. 5 and Fig. S6,† respectively. In both of the EPR spectra, the peaks were broad and featureless without hyperfine splitting. This type of EPR spectrum may indicate that multiple radicals co-exist in the sample or the free radical is not exclusively centered on a single atom.[54] Unresolved hyperfine interactions can contribute to inhomogeneous broadening. Unresolved hyperfine interactions with surrounding nuclei can affect the EPR-line shape and cause broadening of the line width. The *G* values of the EPR spectra of the Ar plasma-treated cellulose and the air plasma-treated cellulose were both 2.0087. The *G* value is generally used to determine the location at which a radical exists. Since the peak is broad and unstructured in both spectra, the measured *G* value can be affected by several radical species that have slightly different *G* values. While a radical in biomass can be carbon-centered or oxygen-centered, a sample containing both carbon-centered and oxygen-centered radicals can also show a single *G* value.[55] In this study, the stability of the free radicals produced during the plasma-pretreatment was further evaluated by storing the freshly treated cellulose in ambient air for different hours. The EPR results of the stored cellulose are also included in Fig. 5 and Fig. S6.† The decrease of the peak intensity along with increasing storage time was observed in both the Ar plasma-treated cellulose and air plasma-treated cellulose. Since the *G* values remain unchanged in the stored cellulose, the free radicals must be converted to nonradical species, probably by reacting with oxygen during the storage.

To determine if the long-lived free radicals present in the plasma pretreatment are related to the increased LG yield, the stored cellulose samples were also pyrolyzed and the LG yields along with the storage times are compared in Fig. 6 for the Ar plasma-pretreated cellulose and in Fig. S7† for the air plasma-pretreated cellulose, both as a function of the storage time. Surprisingly, a gradual decrease of the LG yield with increasing storage times was found for both the Ar plasma-pretreated and air plasma-pretreated cellulose. The presence of a positive correlation between the free radical concentrations remaining in the cellulose and the LG yields suggest that the long-lived free radicals generated by the plasma pretreatment are the key reason for the increased LG yields. Previously, Kuzuya *et al.* also observed long-lived free radicals in Ar plasma-treated

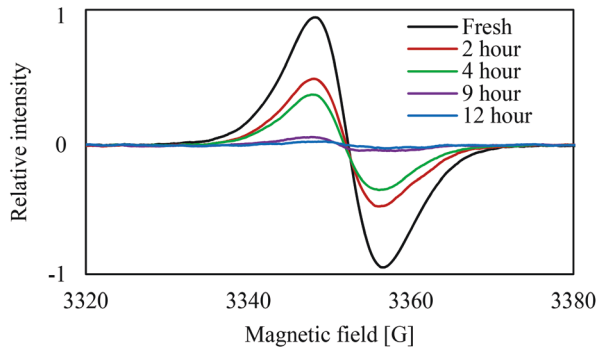

Fig. 5 EPR spectra of the Ar plasma-treated cellulose stored in ambient air for various time. The "fresh" sample was analyzed within 30 min after the plasma treatment (plasma pretreatment conditions: *f* = 17.5 kV, *V* = 2 kHz, and *t* = 30 s.).

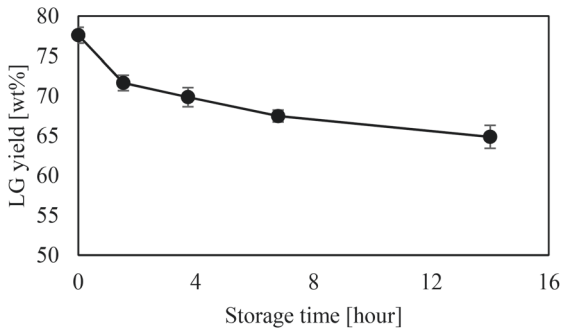

Fig. 6 LG yield obtained from pyrolysis of the Ar plasma-pretreated cellulose stored in ambient air for various time prior to pyrolysis (plasma pretreatment conditions: *f* = 17.5 kV, *V* = 2 kHz, and *t* = 30 s).

cellulose and proposed that the hydrogen abstraction in the pyranose ring produces alkoxy alkyl radicals or hydroxyalkyl radicals inside the ring.[56,57] They noted that the hydroxyalkyl radicals in C2 and C3 were further dehydrated to form more stable acrylic radicals. However, their proposed radicals are unlikely, since such a kind of radical formation cannot cause the chain cleavage or increased cellulose solubility observed in this study. In another study, Hua *et al.* suggested that plasma treatment of cellulose causes pyranosic ring splitting between C1 and C2 to produce two radical fragments.[58] According to their theory, the two radicals further convert to nonradical species containing carbonyl groups at post-treatment by reacting with oxygen. However, the pyranosic ring-opening would result in a decrease in LG yield, which is contradictory to the results of this study. On the other hand, homolytic cleavage of the glycosidic bond and radical formation at the cleaving ends have been proposed in some other studies since this mechanism can explain the decrease of the cellulose DP observed after plasma treatment.[22,54,59,60] Nevertheless, the fate of the glycosidic bond-associated free radicals has not been discussed previously.

The results of this study suggest that radical formation is due to the homolytic cleavage of the glycosidic bond. During the plasma pretreatment, homolytic cleavage could occur in the cellulose midchain to form cellulose (C1)$^{\bullet}$ and cellulose (C4)–O$^{\bullet}$ (indicated as ① and ② in Fig. 7). Other than the two types of radicals, cellulose (C6)–O$^{\bullet}$ (indicated as ③) could also be produced. Previously, Delaux *et al.* synthesized mannose polymers using a nonthermal plasma method and found 71% of the newly formed glycosidic bonds to be either β-1,6 or α-1,6 bonds.[61] Since the polymerization occurred through a radical-based mechanism, their result implies that it is easier to abstract the hydrogen in C6–OH to form C6–O$^{\bullet}$ when a plasma discharge is in effect. In this study, cellulose (C6)–O$^{\bullet}$ could be formed when cellulose (C4)–O$^{\bullet}$ further abstracts the hydrogen in C6–OH in the same glucose unit to form a non-reducing chain end. The formation of cellulose (C6)–O$^{\bullet}$ will weaken interchain hydrogen bonding of the pretreated cellulose. During the plasma treatment, the interchain hydrogen bonding of cellulose could also be weakened due to the electron impact and cellulose chain excitation. Recall that cellulose II was observed in the Ar plasma-treated cellulose due to

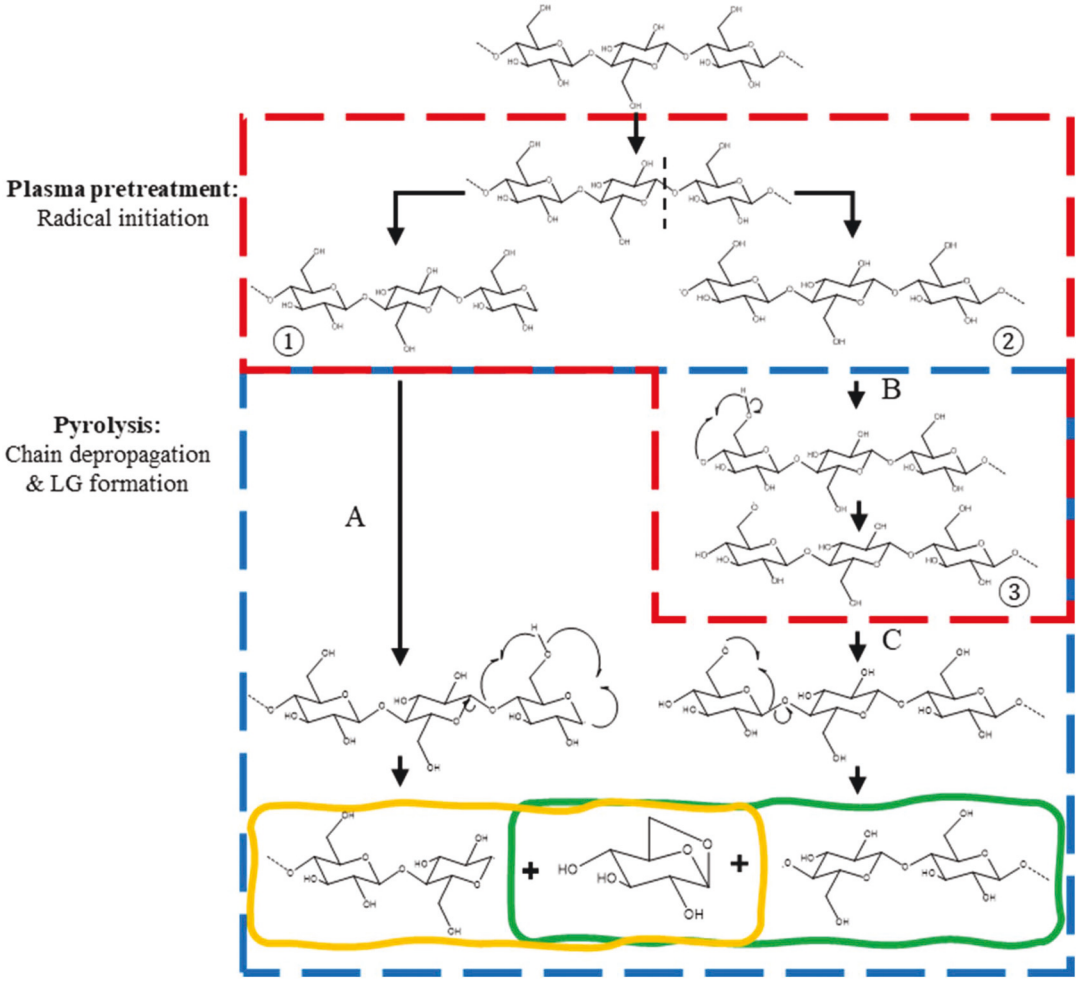

Fig. 7 Radical initiation during the plasma-pretreatment and radical-based chain depropagation during subsequent pyrolysis.

the conformational change. The interchain hydrogen bonding had to be reduced during the pretreatment in order to make such a change. Otherwise, it was impossible for C6–OH to change its conformation in the highly restricted, crystalline structure of cellulose in a solid-state and at a low temperature. The reduced hydrogen bonding could also increase the solubility of the cellulose.[62] On the other hand, the results of the EPR analyses shown above suggest that these free radicals continue to reside in the cellulose after the plasma treatment is completed. Although their high stability and long life span could be the primary reason, radical retention could also be attributed to the uniqueness of the nonthermal plasma technology. Nonthermal plasma discharge barely increased the cellulose temperature despite the fact that it is powerful enough to cause homolytic reactions. Another important feature of nonthermal plasma that is nearly impossible in other thermal-based technologies is that the reactions can be instantly quenched when the energy supply stops. The typical lifetime of excited states is about 10 ns, and thus the depletion process occurs nearly immediately when the energy supply stops.[63] Without a continuous energy supply, the free radicals inside the cellulose at near room temperature could not react further. As a result, the radicals were preserved when the power supply of the plasma reactor was turned off. Other than the above reasons, the densely packed cellulose structure in a solid-state could also have restricted the movement of the radicals.

During the subsequent pyrolysis, these free radicals remaining in the cellulose could start radical-based chain depropagation and LG formation since thermal heating during pyrolysis provides the activation energies of these reactions. According to path A given in Fig. 7, cellulose (C1)$^{\bullet}$ attacks C6–OH in the same glucose unit to form a LG end. During this transposition process, the hydrogen from C6–OH will attack the glycosidic bond to release a LG molecule from the LG end and also form a new cellulose (C1)$^{\bullet}$ with one less DP. In path B, cellulose (C4)–O$^{\bullet}$ abstracts the hydrogen in C6–OH to form cellulose (C6)–O$^{\bullet}$ that has a non-reducing end (or this process may also occur in the plasma treatment as described above). In paths B and C, cellulose (C6)–O$^{\bullet}$ could further attack the glycosidic bond in the chain to form a LG molecule and a new cellulose (C4)–O$^{\bullet}$ with one less DP. These processes repeat until the chain is fully depolymerized. Recall that small amounts of anhydro-oligosaccharides and oligosaccharides were detected from the water-soluble fractions of the pretreated cellulose. The presence of anhydro-oligosaccharides suggests that some of the cellulose (C1)$^{\bullet}$ units further react during the plasma treatment process to turn its radical end into a LG end. However, the above-described chain depropagation and LG formation mainly occurred during the pyrolysis process, since LG was not observed from the water-soluble fraction. The oligosaccharides could be formed when the pretreated cellulose was dispersed in water (for LC-MS analysis) as the free radicals could obtain hydrogen or hydroxyl from water molecules.

It is worth mentioning that several radical-based mechanisms have previously been proposed for cellulose pyrolysis.[22,29] However, the likelihood of the untreated cellulose to depolymerize through a radical-based mechanism is much lower. Firstly, while the homolytic cleavage has a high energy barrier, the untreated cellulose needs to acquire the required activation energy by heat transfer during pyrolysis, which can be challenging. Secondly, as described above, non-radical mechanisms, such as the concerted mechanism and hydroxyl-catalyzed depolymerization, are favored over radical-based mechanisms since they have much lower energy requirements. Nevertheless, only moderate LG yields were obtainable from the pyrolysis of the untreated cellulose, suggesting that these non-radical mechanisms are not very efficient at producing LG from cellulose, as they may compete with other reactions that do not form LG. On the other hand, the energy levels of the excited cellulose chains are high enough that homolytic cleavage of the glycosidic bond could occur, despite the temperature of cellulose remaining very low during the plasma pretreatment. In a radical-based mechanism, the radical propagation step is expected to require a much smaller amount of energy than the initiation step. Thus, radical-based chain depropagation and LG formation could occur during the subsequent pyrolysis of the plasma-pretreated cellulose.

In the following sections, the proposed theories about glycosidic-radical formation during plasma pretreatment and the radical-based mechanism for LG formation during pyrolysis were further investigated.

Pyrolysis of plasma-pretreated saccharides

If the long-lived free radicals derived from glycosidic-bond dissociation promoted the LG yield during cellulose pyrolysis, similar phenomena should also occur to other glycosidic-bond-containing saccharides when pretreated with plasma. To test this hypothesis, glucose, cellobiose, and cellobiosan were also plasma-pretreated in air or Ar and subsequently pyrolyzed. Both cellobiose and cellobiosan contain one glycosidic bond in their molecules, whereas there is no glycosidic bond in glucose. LG yields obtained from the pyrolysis of the saccharides with or without plasma pretreatment are given in Fig. 8. Compared to their untreated counterparts, plasma-pretreated

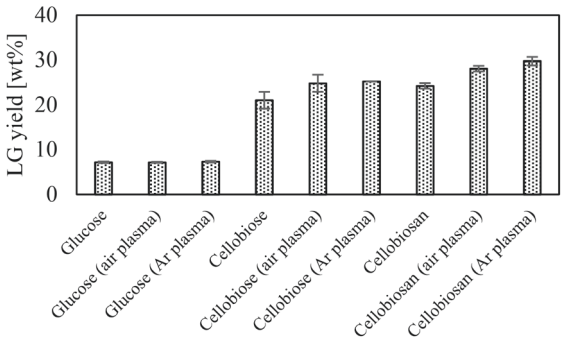

Fig. 8 LG yield obtained from pyrolysis of the untreated and plasma-pretreated saccharides (plasma pretreatment conditions: f = 17.5 kV, V = 2 kHz and t = 30 s for the Ar plasma, and f = 15 kV, V = 2 kHz and t = 30 s for the air plasma).

cellobiose and cellobiosan both produced noticeably higher LG yields. Similar to cellulose, slightly higher LG yields were obtained from the Ar plasma-treated cases than the air plasma-treated cases. In comparison, there were no noticeable changes in the LG yield from the pyrolysis of glucose after the plasma pretreatment. The EPR spectra of plasma-treated cellobiose and glucose were also measured and are shown in Fig. S8.† The EPR result of the Ar plasma-treated cellulose is included in the same figure for comparison. The broad and unstructured peak with a *G* value of 2.0087 previously observed with the plasma-treated cellulose was also found with the plasma-treated cellobiose. However, the peak intensity was much lower in the plasma-treated cellobiose compared to that in the plasma-treated cellulose. The radical concentration is higher in the plasma-treated cellulose due to a large number of glycosidic bonds in the cellulose chain that could be cleaved. The radical concentration in the plasma-treated samples was related to the extent of the LG yield increase in the respective samples. The LG yield increased by 36% (from 57.2% to 77.9%) with cellulose, whereas it increased by 20% in cellobiose (from 21% to 25.2%). On the other hand, the same EPR peak was not observed from the plasma-treated glucose. Therefore, the increase of the LG yield from the plasma-pretreated saccharide samples is clearly associated with the glycosidic bond and the free radical formation during the plasma pretreatment. The radical-based chain depropagation described above is unlikely to occur during the pyrolysis of the plasma-pretreated cellobiose or cellobiosan since their DP is only 2. However, forming glycosidic radicals still promoted LG production better than the original mechanisms for pyrolyzing the untreated cellobiose or cellobiosan.

Co-pyrolysis of plasma-treated cellulose and radical scavenger

As described above, the decreased radical content in the stored cellulose was accompanied by the decreased LG yield during pyrolysis. This is because the decreased number of the initiation radicals reduces the opportunity for the radical-based chain depropagation and LG formation during subsequent pyrolysis. If this hypothesis is correct, co-pyrolyzing plasma-pretreated cellulose with a radical scavenger should also cause a decrease in the LG yield. Thus, hydroquinone was used as the radical scavenging agent and co-pyrolyzed with the Ar plasma-treated cellulose. As given in Fig. 9, the LG yield decreased from 77.9% without hydroquinone to 50.1% with hydroquinone. On the other hand, the LG yield from the co-pyrolysis of the untreated cellulose and hydroquinone was 50.2% compared to 57.2% without hydroquinone. To determine whether hydroquinone caused a secondary reaction of LG to lower its yield, LG was also co-pyrolyzed with hydroquinone. However, this possibility was quickly eliminated since there was no difference in the LG recovery with or without hydroquinone. The intriguing results observed in this study could provide several important insights into cellulose pyrolysis. Firstly, the LG yield decreased by more than 1/3 in the plasma-pretreated cellulose when a radical scavenger was present, which supports our proposed theory about radical-based depolymerization and LG formation of the plasma-pretreated cellulose during pyrolysis. Secondly, the smaller but noticeable decrease of LG yield in the untreated cellulose by the radical scavenging agent may suggest that homolytic cleavage could also occur during the pyrolysis of the untreated cellulose, but only to a small extent. In a previous study, a weak radical peak was observed in the EPR spectra of a cellulose-derived pyrolysis oil.[54] Although the radical(s) in the pyrolysis oil had a different *G* value (*i.e.*, 2.0031), the previous finding still supports the possibility of homolytic cleavage occurring during cellulose pyrolysis. Nonetheless, the LG yield only decreased from 57.2% to 50.2% even after the radical-based pathway was completely blocked (by hydroquinone). Therefore, a non-radical mechanism should be the primary pathway during the pyrolysis of the untreated cellulose. When the untreated cellulose is pyrolyzed, the cellulose chains located on or near the cellulose surface may be able to gain more energy rapidly than the inner chains can. Therefore, homolytic cleavage of the glycosidic bonds may occur sparingly at the surface chains where the higher energy level is reached. However, the chance for the homolytic cleavage to occur is expected to decrease at the inner cellulose chains due to heat transfer limitations. Since the sparingly formed radicals could not penetrate into the inner chains, the inner chains are likely depolymerized by a non-radical mechanism that has a lower energy requirement. In other words, our results suggest that both radical-based and non-radical mechanisms could occur during the pyrolysis of the untreated cellulose, though the non-radical mechanism is the primary pathway. When co-pyrolyzed with hydroquinone, the radical-based mechanism would be inhibited in both the plasma-treated cellulose and untreated cellulose. Therefore, both the plasma-treated cellulose and untreated cellulose depolymerized through a non-radical mechanism in the presence of hydroquinone to produce nearly identical, but lower, yields of LG.

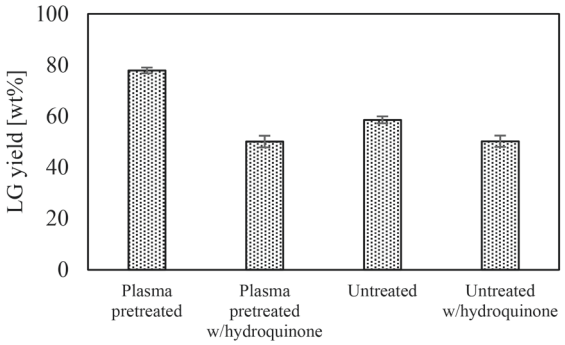

Fig. 9 Comparison of LG yields obtained from pyrolysis of the Ar plasma-pretreated and untreated cellulose in the absence or presence of hydroquinone (plasma pretreatment conditions: f = 17.5 kV, V = 2 kHz, and t = 30 s).

Effect of pyrolysis temperature on LG yield

The TGA results previously given in Fig. 4 show that the plasma-pretreated cellulose decomposes at lower pyrolysis

temperatures. As we described above, the radical initiation took place during the plasma pretreatment. Since the following steps for LG formation do not require as much energy as the radical initiation step, LG could be readily formed using lower pyrolysis temperatures. The weakened interchain hydrogen bonding due to the plasma-induced chain excitation and radical formation may also reduce the decomposition temperatures of the pretreated cellulose. Previously, Hosoya and Sakaki studied cellulose pyrolysis by comparing the activation energy of a single-chain model and a two-chain model to find that the interchain hydrogen bonding increases the activation energy of cellulose depolymerization.[36] Other studies, however, suggest that the interchain hydrogen bonding lowers the activation energy and promotes LG formation during cellulose pyrolysis.[37,38] It is possible that the hydrogen bonding effect is different during the plasma-assisted pyrolysis since the original non-radical mechanism is replaced by the radical-based mechanism. The reduced hydrogen bonding could allow cellulose (C4)–O$^{\bullet}$ to more easily abstract hydrogen at the C6 position or cellulose (C1)$^{\bullet}$ to attack C6–OH to form a C1–O–C6 bridge, therefore promoting the radical-based chain depropagation and LG formation at lower temperatures. To verify the above arguments, the untreated cellulose and Ar plasma-pretreated cellulose were also pyrolyzed at temperatures lower than 450 °C to compare LG yields (Fig. 10). The LG yield from the pretreated cellulose was 63.2% at 350 °C and rapidly increased to 77.6% at 375 °C. At temperatures above 375 °C, the LG yields basically remain unchanged with the maximum yield of 78.6% occurring at 425 °C. In comparison, the LG yields from pyrolysis of the untreated cellulose were only 51.7% and 53.2% at 350 °C and 375 °C, respectively, with the maximum yield of 58.2% at 400 °C.

Overall, our experimental results support the proposed theories about the role of plasma pretreatment in LG production. Nevertheless, there are optimum pretreatment conditions in order to obtain the highest LG yield. During plasma treatment, the amount of energy transferred to the cellulose depends on the density of free electrons and their energy levels, which are determined from the parameters of the AC power supply and plasma treatment time. Plasma charge that is too weak or treatment time that is too short may not provide sufficient energy for the homolytic cleavage of the glycosidic bonds, whereas plasma discharge that is too strong or treatment time that is too long may also cause homolytic cleavage of the carbon–carbon or carbon–oxygen bonds inside the pyranosic ring. The feed gas also has an effect since it can change the composition of the plasma discharge. When cellulose was plasma-treated in air, ozone and oxygen radicals generated by the plasma discharge may have slightly caused ring-opening reactions and oxidation reactions,[64] though they were not noticeable based on the FTIR results given above. The negative effect caused by the oxidation agents is expected to become more significant with higher AC power and longer pretreatment time. Therefore, not only was the optimum LG yield slightly lower, but the decline of LG yields at prolonged pretreatment times or with higher power conditions were also more noticeable with the air plasma-treated cellulose.

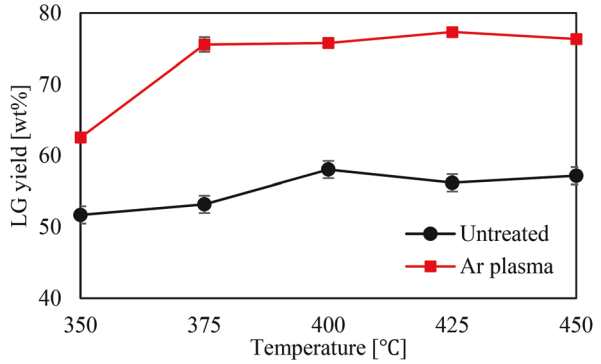

Fig. 10 LG yields obtained from the untreated and Ar plasma-pretreated cellulose using different pyrolysis temperatures (plasma pretreatment conditions: f = 17.5 kV, V = 2 kHz, and t = 30 s).

Conclusions

In this study, LG yield from cellulose pyrolysis was increased from a maximum of 58.2% up to 78.6% by pretreating cellulose with atmospheric pressure nonthermal plasma. While pretreatments with both Ar plasma and air plasma were effective, the Ar plasma pretreatment delivered slightly better results than the air plasma-pretreatment. It was found that the plasma treatment causes homolytic cleavage of the glycosidic bonds to form free radicals. During the subsequent pyrolysis, the free radicals remaining in the plasma-pretreated cellulose enabled radical-based chain depropagation and LG formation. The present study also suggests that while the radical-based mechanism is more effective at forming LG, pyrolysis of the untreated cellulose mainly occurs through a non-radical mechanism hindered by the high energy barrier of homolytic cleavage. On the other hand, the combination of the plasma pretreatment and subsequent pyrolysis enabled the transition from the non-radical mechanism to the radical-based mechanism. This change also allowed the plasma-pretreated cellulose to produce higher yields of LG using lower pyrolysis temperatures. At 375 °C, the LG yield from the Ar plasma-pretreated cellulose was 77.6% compared to 53.2% from the untreated cellulose. The energy requirement at the radical-based chain depropagation and LG steps is expected to be lower than that at the radical initiation step, causing the plasma-pretreated cellulose to depolymerize at lower temperatures. The plasma-induced chain excitement and radical formation could also have reduced interchain hydrogen bonding to lower the energy requirement during the subsequent pyrolysis.

Conflicts of interest

There are no conflicts to declare.

Acknowledgements

The authors would like to acknowledge Dr Sarah Cady and Dr Kamel Harrata in the Department of Chemistry at Iowa State University for technical support in the EPR and LC-MS analyses. The authors also acknowledge the instrumental support from Bioeconomic Institute and Dr Hui Hu from the Department of Aerospace Engineering, both at Iowa State University. This research is partially supported by National Science Foundation Grants No. 1826978 and 1803823.

References

1 P. McKendry, *Bioresour. Technol.*, 2002, **83**, 37–46.
2 D. Mohan, C. U. Pittman and P. H. Steele, *Energy Fuels*, 2006, **20**, 848–889.
3 S. H. Krishna, K. Huang, K. J. Barnett, J. He, C. T. Maravelias, J. A. Dumesic, G. W. Huber, M. De Bruyn and B. M. Weckhuysen, *AIChE J.*, 2018, **64**, 1910–1922.
4 F. Jérôme, G. Chatel and K. De Oliveira Vigier, *Green Chem.*, 2016, **18**, 3903–3913.
5 J. Vanneste, T. Ennaert, A. Vanhulsel and B. Sels, *ChemSusChem*, 2017, **10**, 14–31.
6 K. H. Becker, U. Kogelschatz, K. H. Schoenbach, R. J. Barker, U. Kogelschatz, K. H. Schoenbach and R. J. Barker, *Non-Equilibrium Air Plasmas at Atmospheric Pressure*, CRC Press, 2004.
7 K. Weltmann, J. F. Kolb, M. Holub, D. Uhrlandt, M. Šimek, K. (Ken) Ostrikov, S. Hamaguchi, U. Cvelbar, M. Černák, B. Locke, A. Fridman, P. Favia and K. Becker, *Plasma Processes Polym.*, 2019, **16**, 1800118.
8 A. Bogaerts, E. Neyts, R. Gijbels and J. Van der Mullen, *Spectrochim. Acta, Part B*, 2002, **57**, 609–658.
9 J. A. Souza-Corrêa, C. Oliveira, L. D. Wolf, V. M. Nascimento, G. J. M. Rocha and J. Amorim, *Appl. Biochem. Biotechnol.*, 2013, **171**, 104–116.
10 N. Schultz-Jensen, Z. Kádár, A. B. Thomsen, H. Bindslev and F. Leipold, *Appl. Biochem. Biotechnol.*, 2011, **165**, 1010–1023.
11 W. Zhao, J. Huang, K. Ni, X. Zhang, Z. Lai, Y. Cai and X. Li, *J. Energy Inst.*, 2018, **91**, 595–604.
12 H. Taghvaei and M. R. Rahimpour, *Process Saf. Environ. Prot.*, 2019, **121**, 221–228.
13 M. Benoit, A. Rodrigues, Q. Zhang, E. Fourré, K. De Oliveira Vigier, J.-M. M. Tatibouët and F. Jérôme, *Angew. Chem., Int. Ed.*, 2011, **50**, 8964–8967.
14 M. Benoit, A. Rodrigues, K. De Oliveira Vigier, E. Fourré, J. Barrault, J.-M. M. Tatibouët and F. Jérôme, *Green Chem.*, 2012, **14**, 2212.
15 T. Werpy and G. Petersen, *Top Value Added Chemicals from Biomass: Volume I – Results of Screening for Potential Candidates from Sugars and Synthesis Gas*, Golden, CO, United States, 2004.
16 Z. Chi, M. Rover, E. Jun, M. Deaton, P. Johnston, R. C. Brown, Z. Wen and L. R. Jarboe, *Bioresour. Technol.*, 2013, **150**, 220–227.
17 J. Lian, M. Garcia-Perez and S. Chen, *Bioresour. Technol.*, 2013, **133**, 183–189.
18 S. Maduskar, V. Maliekkal, M. Neurock and P. J. Dauenhauer, *ACS Sustainable Chem. Eng.*, 2018, **6**, 7017–7025.
19 N. Kuzhiyil, D. Dalluge, X. Bai, K. H. Kim and R. C. Brown, *ChemSusChem*, 2012, **5**, 2228–2236.
20 A. Ghosh, R. C. Brown and X. Bai, *Green Chem.*, 2016, **18**, 1023–1031.
21 A. Ghosh, X. Bai and R. C. Brown, *ChemistrySelect*, 2018, **3**, 4777–4785.
22 H. B. Mayes and L. J. Broadbelt, *J. Phys. Chem. A*, 2012, **116**, 7098–7106.
23 J. K. Lindstrom, J. Proano-Aviles, P. A. Johnston, C. A. Peterson, J. S. Stansell and R. C. Brown, *Green Chem.*, 2019, **21**, 178–186.
24 P. R. Patwardhan, J. A. Satrio, R. C. Brown and B. H. Shanks, *J. Anal. Appl. Pyrolysis*, 2009, **86**, 323–330.
25 V. Mamleev, S. Bourbigot, M. Le Bras and J. Yvon, *J. Anal. Appl. Pyrolysis*, 2009, **84**, 1–17.
26 J. Lédé, *J. Anal. Appl. Pyrolysis*, 2012, **94**, 17–32.
27 P. J. Dauenhauer, J. L. Colby, C. M. Balonek, W. J. Suszynski and L. D. Schmidt, *Green Chem.*, 2009, **11**, 1555–1561.
28 C. Krumm, J. Pfaendtner and P. J. Dauenhauer, *Chem. Mater.*, 2016, **28**, 3108–3114.
29 D. K. Shen and S. Gu, *Bioresour. Technol.*, 2009, **100**, 6496–6504.
30 G. R. Ponder and G. N. Richards, *Biomass Bioenergy*, 1994, **7**, 1–24.
31 T. L. Lowary and G. N. Richards, *Carbohydr. Res.*, 1990, **198**, 79–89.
32 A. G. W. Bradbury, Y. Sakai and F. Shafizadeh, *J. Appl. Polym. Sci.*, 1979, **23**, 3271–3280.
33 B. Zhang, E. Leng, Y. Wang, X. Gong, Y. Zhang and M. Xu, *BioResources*, 2017, **12**, 2731–2747.
34 T. Hosoya, Y. Nakao, H. Sato, H. Kawamoto and S. Sakaki, *J. Org. Chem.*, 2009, **74**, 6891–6894.
35 V. Seshadri and P. R. Westmoreland, *J. Phys. Chem. A*, 2012, **116**, 11997–12013.
36 T. Hosoya and S. Sakaki, *ChemSusChem*, 2013, **6**, 2356–2368.
37 E. Leng, Y. Zhang, Y. Peng, X. Gong, M. Mao, X. Li and Y. Yu, *Fuel*, 2018, **216**, 313–321.
38 V. Maliekkal, S. Maduskar, D. J. Saxon, M. Nasiri, T. M. Reineke, M. Neurock and P. Dauenhauer, *ACS Catal.*, 2019, **9**, 1943–1955.
39 P. R. Patwardhan, J. A. Satrio, R. C. Brown and B. H. Shanks, *Bioresour. Technol.*, 2010, **101**, 4646–4655.
40 X. Bai, P. Johnston, S. Sadula and R. C. Brown, *J. Anal. Appl. Pyrolysis*, 2013, **99**, 58–65.
41 P. R. Patwardhan, D. L. Dalluge, B. H. Shanks and R. C. Brown, *Bioresour. Technol.*, 2011, **102**, 5265–5269.
42 F. Ronsse, X. Bai, W. Prins and R. C. Brown, *Environ. Prog. Sustainable Energy*, 2012, **31**, 256–260.

43 J. Proano-Aviles, J. K. Lindstrom, P. A. Johnston and R. C. Brown, *Energy Technol.*, 2017, **5**, 189–195.

44 A. D. Paulsen, M. S. Mettler and P. J. Dauenhauer, *Energy Fuels*, 2013, **27**, 2126–2134.

45 M. S. Mettler, A. D. Paulsen, D. G. Vlachos and P. J. Dauenhauer, *Green Chem.*, 2012, **14**, 1284–1288.

46 J. Zhang, M. W. Nolte and B. H. Shanks, *ACS Sustainable Chem. Eng.*, 2014, **2**, 2820–2830.

47 Z. Wang, A. G. McDonald, R. J. M. Westerhof, S. R. A. Kersten, C. M. Cuba-Torres, S. Ha, B. Pecha and M. Garcia-Perez, *J. Anal. Appl. Pyrolysis*, 2013, **100**, 56–66.

48 J.-F. Revol and D. A. I. Goring, *J. Appl. Polym. Sci.*, 1981, **26**, 1275–1282.

49 M. Takahashi and H. Takenaka, *Polym. J.*, 1987, **19**, 855–861.

50 C. M. G. Carlsson and G. Stroem, *Langmuir*, 1991, **7**, 2492–2497.

51 K. Kolářová, V. Vosmanská, S. Rimpelová and V. Švorčík, *Cellulose*, 2013, **20**, 953–961.

52 M. G. McCord, Y. J. Hwang, Y. Qiu, L. K. Hughes and M. A. Bourham, *J. Appl. Polym. Sci.*, 2003, **88**, 2038–2047.

53 H. Taghvaei and M. R. Rahimpour, *J. Anal. Appl. Pyrolysis*, 2018, **135**, 422–430.

54 K. H. Kim, X. Bai, S. Cady, P. Gable and R. C. Brown, *ChemSusChem*, 2015, **8**, 894–900.

55 K. H. Kim, X. Bai and R. C. Brown, *J. Anal. Appl. Pyrolysis*, 2014, **110**, 254–263.

56 M. Kuzuya, K. Morisaki, J. Niwa, Y. Yamauchi and K. Xu, *J. Phys. Chem.*, 1994, **98**, 11301–11307.

57 M. Kuzuya, N. Noda, S. Kondo, K. Washino and A. Noguchi, *J. Am. Chem. Soc.*, 1992, **114**, 6505–6512.

58 Z. Q. Hua, R. Sitaru, F. Denes and R. A. Young, *Plasmas Polym.*, 1997, **2**, 199–224.

59 N. S. Hon, *J. Polym. Sci., Polym. Chem. Ed.*, 1976, **14**, 2497–2512.

60 I. P. Edimecheva, R. M. Kisel, O. I. Shadyro, K. Kazem, H. Murase and T. Kagiya, *J. Radiat. Res.*, 2005, **46**, 319–324.

61 J. Delaux, M. Nigen, E. Fourré, J.-M. Tatibouët, A. Barakat, L. Atencio, J. M. García Fernández, K. De Oliveira Vigier and F. Jérôme, *Green Chem.*, 2016, **18**, 3013–3019.

62 W. W. Jun, Z. Fengcai and C. Bingqiang, *Plasma Sci. Technol.*, 2008, **10**, 743–747.

63 T. Von Woedtke, A. Schmidt, S. Bekeschus, K. Wende and K.-D. Weltmann, *In Vivo*, 2019, **33**, 1011–1026.

64 A. Calvimontes, P. Mauersberger, M. Nitschke, V. Dutschk and F. Simon, *Cellulose*, 2011, **18**, 803–809.

Electronic Supplementary Material (ESI) for Green Chemistry.

SUPPORTING INFORMATION

Producing High Yield of Levoglucosan by Pyrolyzing Non-thermal Plasma-Pretreated Cellulose

Lusi A[1], Haiyang Hu[2], Xianglan Bai[1]*

[1]Department of Mechanical Engineering, Iowa State University, Ames, IA 50011 USA

[2]Department of Aerospace Engineering, Iowa State University, Ames, IA 50011 USA

*Corresponding author, Email: bxl9801@iastate.edu

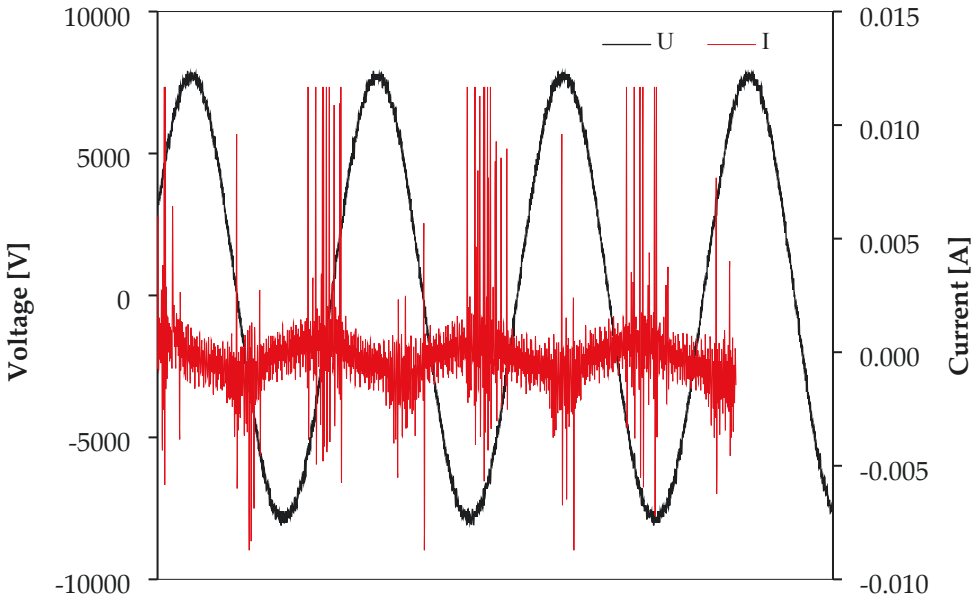

Fig S1. Voltage-current graph during plasma treatment

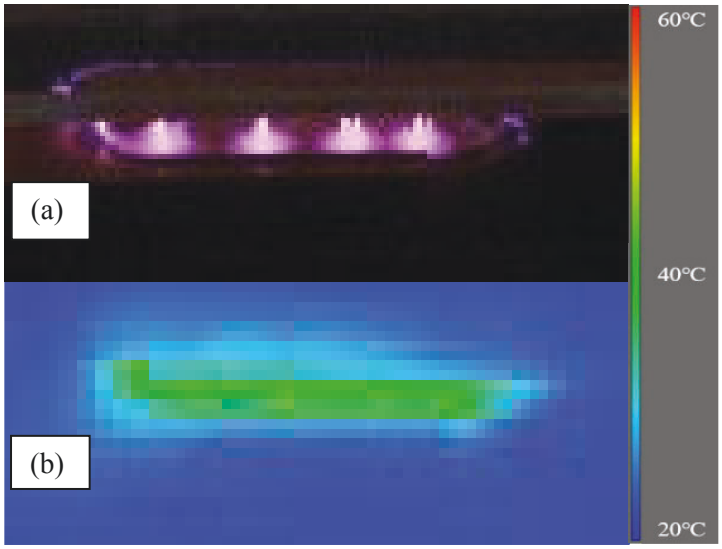

Fig S2 (a). Snapshot of cellulose under plasma treatment; (b). IR thermographic image for temperature distribution after 5 min. The temperature scale is shown in the right side bar.

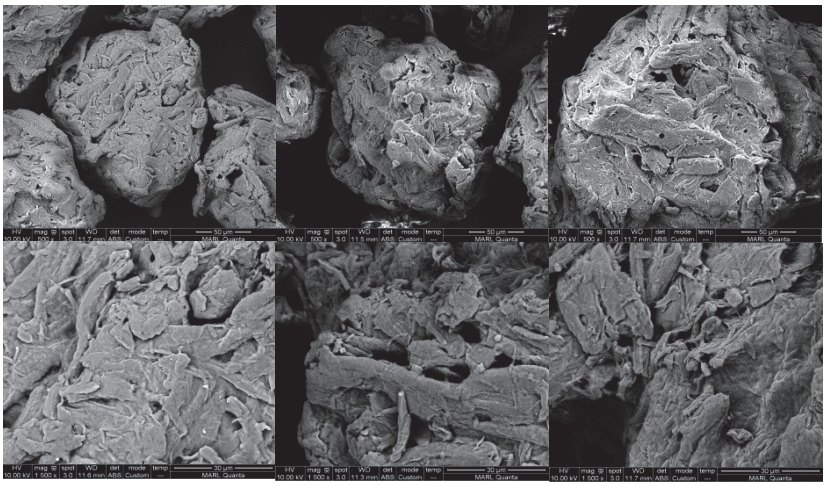

Untreated Ar plasma Air plasma

Fig S3. SEM images of the untreated and plasma-pretreated cellulose. The AC power condition and pretreatment time are f = 17.5 kV, V = 2 kHz and t = 30 s for the Ar plasma-treated cellulose, and f = 15 kV, V = 2 kHz and t = 30s for the air plasma-treated cellulose.

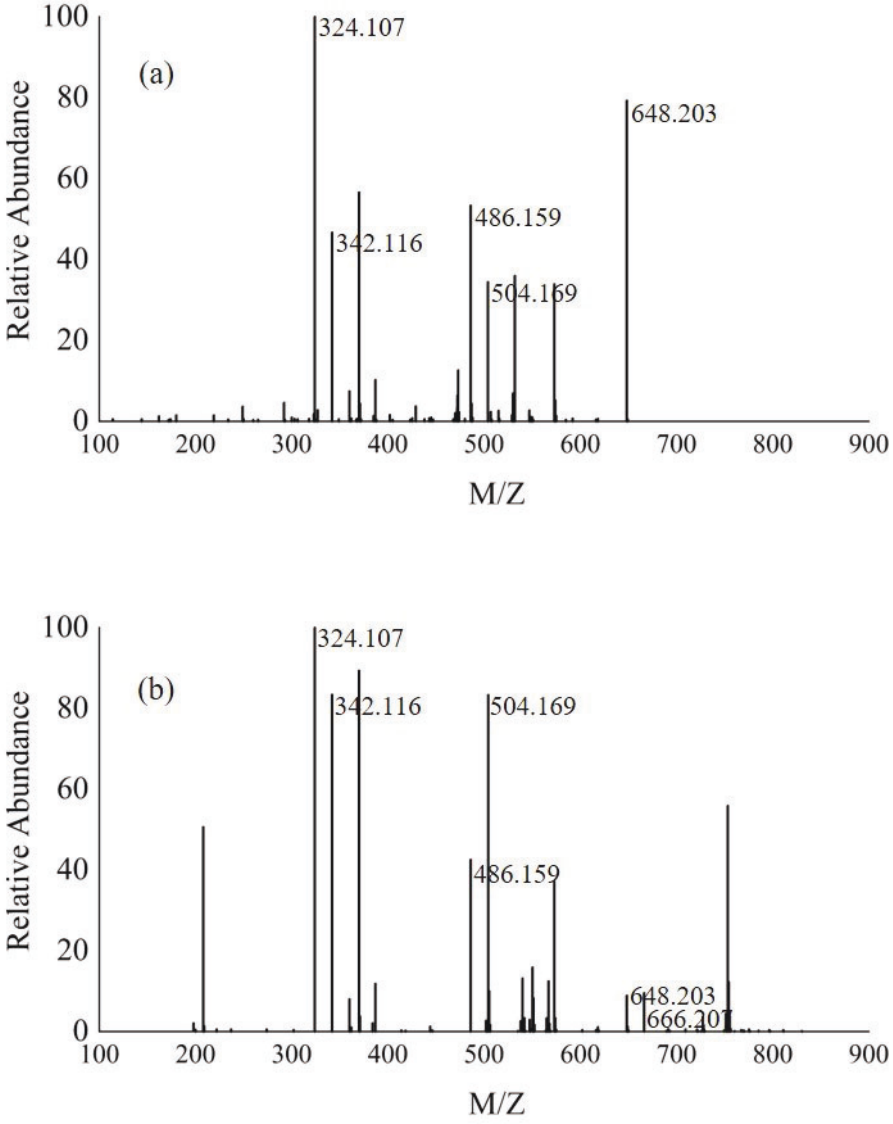

Fig S4. LC-MS results of the water-soluble fractions of the plasma pretreated cellulose. (a). the Air plasma pretreated cellulose, (b). the Ar plasma pretreated cellulose. (Plasma pretreatment conditions are f = 17.5 kV, V = 2 kHz and t = 30s for the Ar plasma, and f = 15 kV, V = 2 kHz and t = 30 s for the air plasma.)

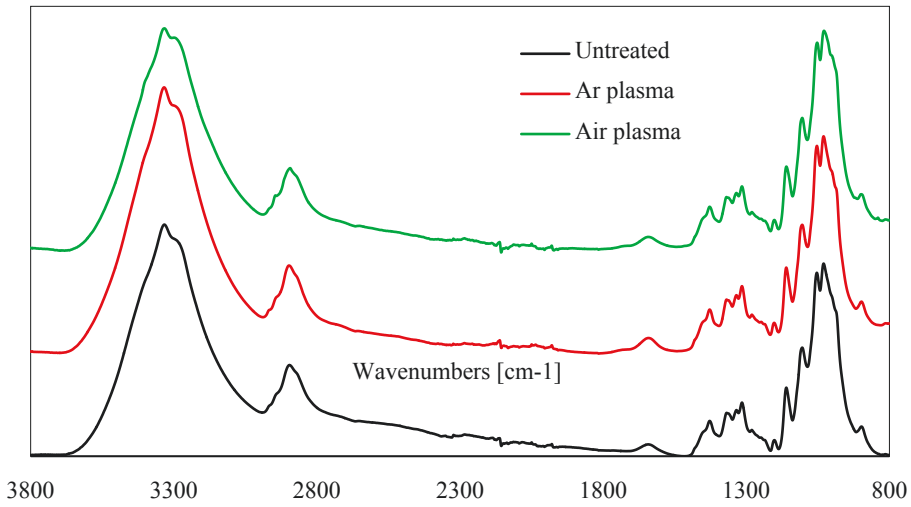

Fig S5. FTIR spectra of the untreated and plasma-pretreated cellulose. (Plasma pretreatment conditions are f = 17.5 kV, V = 2 kHz and t = 30 s for the Ar plasma, and f = 15 kV, V=2 kHz and t = 30 s for the air plasma.)

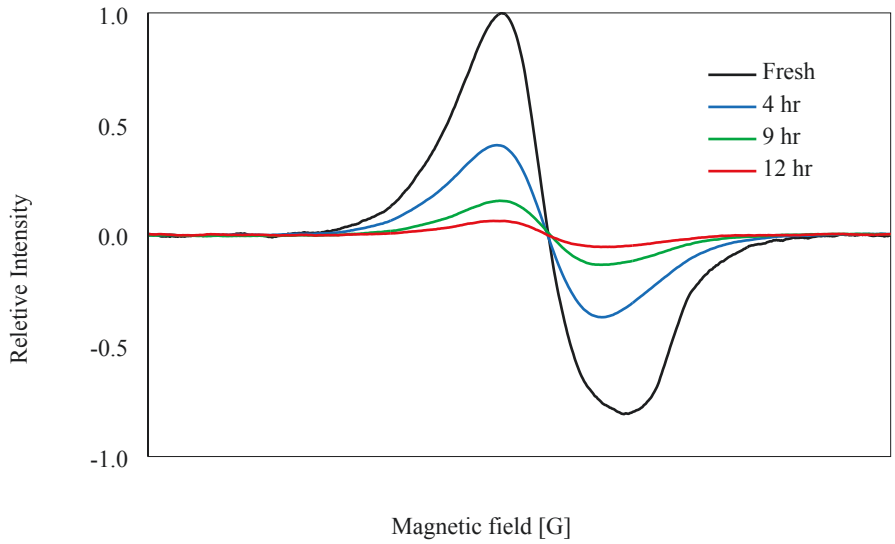

Fig S6. EPR spectra of the air plasma-pretreated cellulose stored at ambient air for various times. The "Fresh" sample was analyzed within 30 min after the plasma treatment. (Plasma pretreatment conditions: f = 15 kV, V = 2 kHz, t = 30 s.)

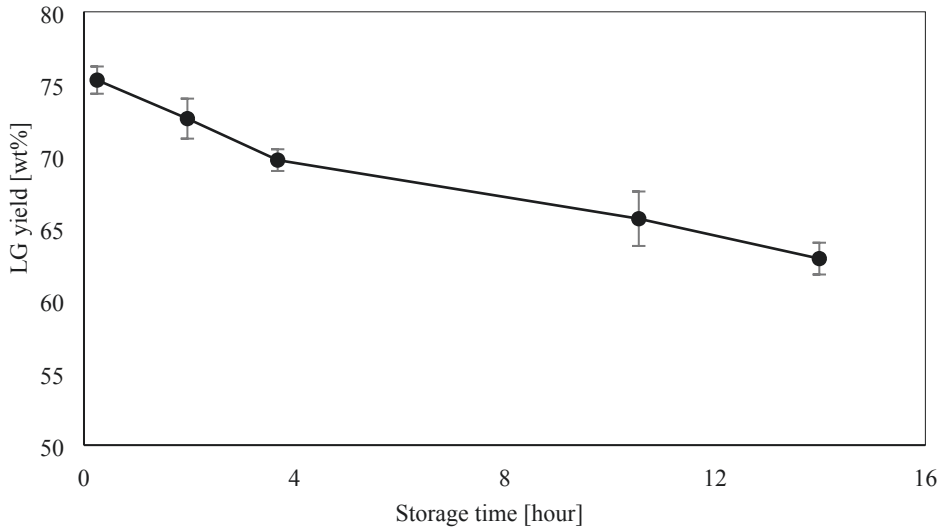

Fig S7. LG yield produced from pyrolysis of the air plasma-pretreated cellulose stored at ambient air for various times prior to pyrolysis. (Plasma pretreatment conditions: f = 15 kV, V = 2 kHz, t = 30 s.)

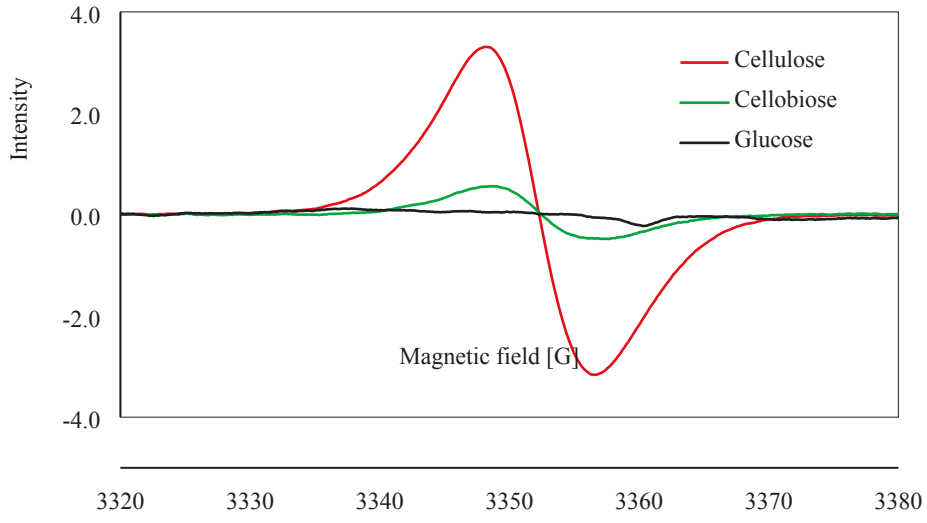

Fig S8. EPR spectra of the Ar plasma-pretreated cellulose and saccharides. (Plasma pretreatment conditions: f = 17.5 kV, V = 2 kHz, t = 30 s.)